JOURNAL OF APPLIED ELECTROCHEMISTRY 17 (1987) 1093–1099

Potentiostatic study of the electrochemical nucleation of oxide films on cadmium in alkaline solutions

J. A. GARRIDO, F. CENTELLAS, P. Ll. CABOT, R. M. RODRÍGUEZ, E. PÉREZ

Departament de Química Física, Facultat de Química, Universitat de Barcelona, Avda. Diagonal, 647, 08028-Barcelona, Spain

Received 2 December 1986; revised 18 February 1987

A potentiostatic study of polycrystalline cadmium anodes (99.99%) in KOH solutions has been performed. The corresponding I–t curves obtained for potentials between -840 and -890 mV (versus Hg/HgO, KOH_{sln}) show a minimum and a maximum of current for all the concentrations of KOH employed, except for 0.5 M.

The mathematical treatment applied to the region appearing after the current minimum suggests that the cadmium oxide growth on the metal takes place according to a diffusion-controlled, three-dimensional hemispherical electrocrystallization with progressive nucleation. However, a change in the type of nucleation must be accepted, from progressive for short times to instantaneous for larger times. This change is more pronounced when the KOH concentration increases and explains the (I^2/J_m^2) versus (t/t_m) and the log I versus log t plots established for the different models of electrocrystallization.

1. Introduction

The electrochemical behaviour of cadmium electrodes in alkaline solutions has been the object of many studies because of the wide application of the metal in batteries. A great number of these works deal with the anodic behaviour of cadmium in alkaline solutions. The lack of uniform criteria on the species formed and the mechanism of the anodic oxidation justified systematic work on the electrochemical behaviour of this electrode in different solutions of potassium hydroxide [1–3], using potentiostatic and potentiodynamic [1] and galvanostatic techniques [2, 3]. These electrochemical techniques, together with further auxiliary methods (electron and X-ray diffraction, scanning electron microscopy, etc.), are the most commonly employed techniques in the study of metal oxidation.

In the earlier work [1–3] the potentiodynamic curves obtained showed a sharp maximum (A) in the anodic region, followed by a further, blunter one (B) and then by a passivation zone. In the cathodic region only one sharp peak (C) was observed. The current density of the peaks increased linearly with the square root of the sweep rate. The peak potentials did not vary at low sweeping speeds, but at higher values they showed a variation which was linearly dependent on the logarithm of the sweep rate. From the potentiostatic curves in the anodic range at short times, we obtained applied overpotential versus logarithm current density plots at zero time, which followed the Tafel relation. On the other hand, from the variation in the value of η ($t = 0$) with applied current density, the Tafel plots for the anodic and cathodic galvanostatic plateaux were obtained. The results obtained by using these techniques permitted postulation of a mechanism for the formation of a film, composed of $Cd(OH)_2$ and CdO, during the anodic oxidation process. The initial film, which is formed through a dissolution–precipitation mechanism, as found from the galvanostatic technique, increases in $Cd(OH)_2$ content with respect to its content in CdO. It was also suggested that such a film continues to grow three-dimensionally,

0021–891X/87 $03.00 + .12 © 1987 Chapman and Hall Ltd.

the corresponding ionic species being transported through the pores in the initial film. During the cathodic process, the stoichiometric relation between the quantity of CdO and $Cd(OH)_2$ reduced varies with the KOH concentration, a greater quantity of CdO than $Cd(OH)_2$ being reduced when the KOH concentration increases.

The aim of the present work is to find a valid mathematical model for cadmium oxide growth in alkaline media in order to interpret the experimental results and also other recent data on electroformed species and its mechanism of formation on metal surfaces. Therefore, the potentiostatic oxidation of a cadmium polycrystalline electrode in KOH solutions at potentials corresponding to the oxide formation has been performed. In order to study the effect of pH changes on the growth law, several KOH concentrations have been employed.

2. Experimental details

The experiments were performed using a polycrystalline cadmium rod (99.99% pure, Merck), having a diameter of 9.5 mm, placed in a vertical cell which allowed electrolyte circulation and N_2 bubbling through the working solution. The counter and reference electrodes were, respectively, a platinum mesh, with an area about 10 times greater than the section of the working electrode, and a (Hg/HgO, KOH_{sln}) reference electrode, the latter connected via a Luggin capillary. All the potentials given in this work are referred to this reference electrode. The electrochemical cell and the electrodes used in this work have been described previously [1].

The experiments were performed by means of a mod. 551 AMEL potentiostat–galvanostat and the resulting curves recorded and measured on a 3091 Nicolet digital storage oscilloscope and transferred to an X–Y recorder and also to a LY-1800 Linseis X–Y recorder.

The electrolyte used was AR grade Merck KOH, free of carbonates, and the concentrations employed were 0.5, 1.0, 1.2, 1.4, 1.7, 2.0 and 2.2 mol dm^{-3} (titrated against potassium acid phthalate of AR grade Merck quality). All the solutions were prepared with deionized and doubly distilled water, recently purified by means of a Millipore Milli-Q system. The temperature was maintained at 25.0 ± 0.1° C for all the experiments.

Before each experimental determination, the cadmium polycrystalline electrode was polished, degreased and washed repeatedly with ethanol and Milli-Q water and also cathodically polarized at −1450 mV versus (Hg/HgO, KOH_{sln}) for 2 min in order to reduce possible oxide residues on the metal surface, and then the selected potential was applied.

3. Results

The general form of the potentiostatic curves obtained are of two different types which are shown in Fig. 1. The experimental curves exhibit one or the other form depending both on the potential applied and the concentration of the electrolyte. In all the cases, the potentials studied cover the range between −840 mV versus (Hg/HgO, KOH_{sln}) and the rest potential of the electrode in the working solution. These potentials correspond to the potentiodynamic peak A (cf. [1]) where the cadmium oxides are formed. Thus, the experimental curves obtained at low overpotentials are similar to that shown in Fig. 1b, while those obtained at high overpotentials exhibit the form indicated in Fig. 1a. However, there is an exception for low concentrations (0.5 mol dm^{-3}), because in this case, all the potentiostatic curves are similar to that corresponding to Fig. 1a. Curves of the type shown in Fig. 1b have been also found for copper [4, 5] and tin [6] and are typical of electrocrystallization processes.

A study of the potentiostatic curves at short times was performed in a previous paper [1]. In the present work, the zone of these curves

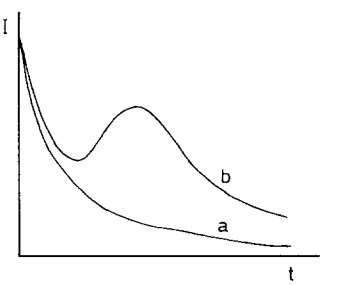

Fig. 1. General form of the I–t curves obtained.

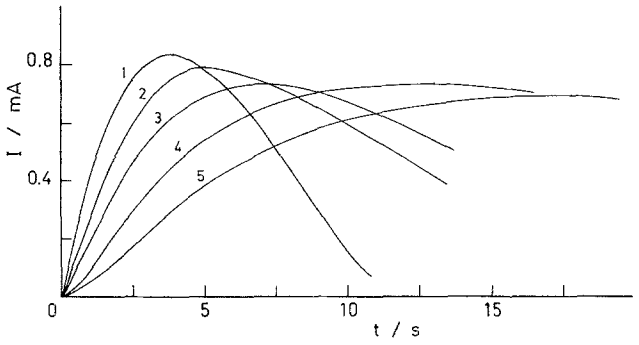

Fig. 2. Potentiostatic current–time transients, referred to the corresponding minimum current, for the 2.2 mol dm^{-3} KOH solution (see text). Potential applied (mV): 1, −867; 2, −871; 3, −875, 4, −880; 5, −883. Electrode area, 0.71 cm^2.

between the minimum and the maximum value of the current (see Fig. 1b) is the object, this zone corresponding to a crystal growth process. This formation of crystals has been shown experimentally by means of electron and X-ray diffraction and scanning electron microscopy (SEM) [7–11]. Therefore, the current of the experimental curves has been measured as a function of time taking as the origin the minimum value of the current, since it is from this point that crystal growth has been demonstrated by SEM [12]. In Fig. 2, several of these curves obtained for the 2.2 mol dm^{-3} KOH solution are shown from the corresponding minimum current.

4. Discussion

The treatment of the experimental curves for the region after the minimum value of the current has been performed in the light of the models developed for the formation of deposits by multiple nucleation and subsequent growth of the nuclei. In the electrocrystallization models, the mathematical equations obtained for the current depend on the type of nucleation taking place on the electrode and on the geometrical model considered for the film growth. For both a two-dimensional or a hemispherical three-dimensional growth of the nuclei and short times, the general equation for the intensity of current, when the nucleation rate constant, A, is great with respect to the time of the process (that is, when instantaneous nucleation takes place) can be written in two simple limit forms [13–16]:

$$I = 2\pi zF(M/\varrho)hk^2N_0t \qquad (1)$$

for a two-dimensional growth and

$$I = 2\pi zF(M/\varrho)^2k^3N_0t^2 \qquad (2)$$

for a three-dimensional hemispherical growth of the nuclei, where k represents the rate constant of the crystal growth, N_0 the number of growing nuclei initially on the metal surface and ϱ the density of the film formed. If the nucleation constant is low compared with the time of the process a progressive nucleation takes place, the result being in this case:

$$I = 2\pi zF(M/\varrho)hk^2AN_0t^2 \qquad (3)$$

for a two-dimensional growth and

$$I = (2\pi/3)zF(M/\varrho)^2k^3AN_0t^3 \qquad (4)$$

when the nuclei growth is hemispheric and three-dimensional.

In these types of treatment it is assumed that the growth of the nuclei takes place in an independent form, this fact being probably true in the initial stages. If this is the case, the age and the state of growth of the aforementioned nuclei is similar. Therefore, such equations are only valid for short times and when the time of growth is sufficiently high, these nuclei overlap and the nucleation rate decreases.

These models have been applied with success to copper [5] and tin [6]. However, none of these latter models can be applied to the present case because the I versus t, I versus t^2 and I versus t^3 plots did not lead to satisfactory results (no straight lines were found).

Hills and co-workers [16–18] have shown that for a diffusion-controlled, hemispherical, three-dimensional growth of the crystals, the net current can be expressed as

$$I = \frac{zF\pi(2Dc)^{\frac{3}{2}}M^{\frac{1}{2}}N}{\varrho^{\frac{1}{2}}}t^{\frac{1}{2}} \qquad (5)$$

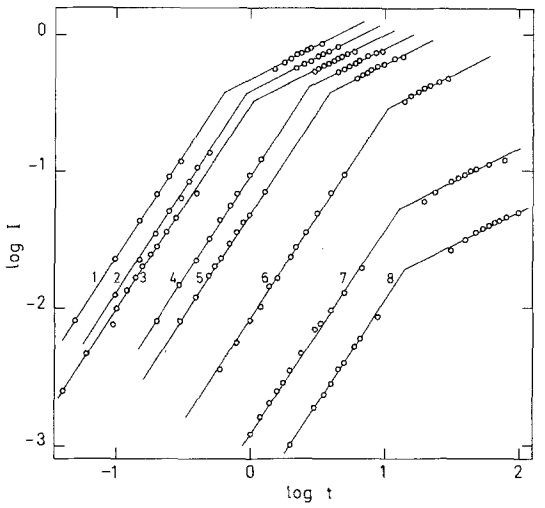

Fig. 3. Log I versus log t plots for the 2.2 mol dm^{-3} KOH solution. Potential applied (mV): 1, −867; 2, −871; 3, −875; 4, −880; 5, −883; 6, −885; 7, −887; 8, −889.

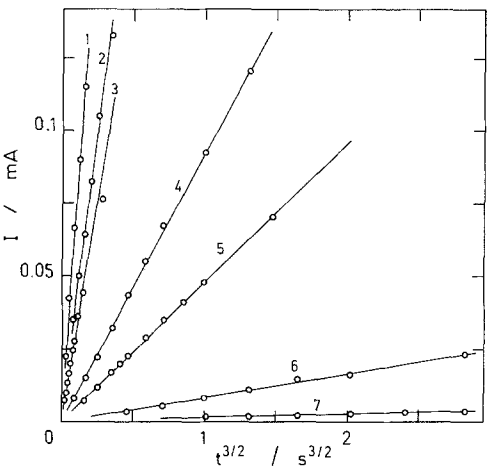

Fig. 4. Plot of I against $t^{\frac{3}{2}}$ for transients obtained for the 2.2 mol dm^{-3} KOH solution. Potential applied (mV): 1, −867; 2, −871; 3, −875; 4, −880; 5, −883; 6, −885; 7, −887.

when the nucleation is instantaneous and

$$I = \frac{2zF\pi(2Dc)^{\frac{3}{2}}M^{\frac{1}{2}}AN_{\infty}}{3\varrho^{\frac{1}{2}}} t^{\frac{3}{2}} \qquad (6)$$

for a progressive nucleation, D being the diffusion coefficient and c, the bulk concentration of the species involved. The other parameters have their normal meaning in electrocrystallization theory.

Equations 1–6, even though they are approximate forms of more complex equations (which can be applied for longer time ranges), are useful tools for testing the models and allow study of the mechanism of the crystal growth.

In order to study the validity of the diffusion-controlled model in the system described in the present work, double logarithmic plots, i.e. log I versus log t, have been drawn for each potential. The resulting curves are of the type shown in Fig. 3, which corresponds to the 2.2 mol dm^{-3} KOH solution. In these plots, two different linear regions can be clearly discerned. The first has a slope of $\frac{3}{2}$ and corresponds to a zone of the potentiostatic curve near the minimum value of the current. The second linear region exhibits a slope of $\frac{1}{2}$ and corresponds to times somewhat greater than that corresponding to the minimum of the experimental I–t curve. These dependences are valid for sufficiently long times, for example 7s in the first linear region and 49s in the second linear region when the applied potential is −889 mV and the KOH concentration is 2.2 mol dm^{-3}, thus justifying the origin of coordinates taken in Fig. 2. Similar behaviour has been found for the other KOH solutions employed and applied potentials leading to a maximum value of the current in the potentiostatic curves.

Plots of I versus $t^{3/2}$ and versus $t^{1/2}$ have also been obtained for all the concentrations of KOH used and the potentials applied in this work. The curves corresponding to the 2.2 mol dm^{-3} KOH solution are shown in Figs 4 and 5. Again, two linear regions can be clearly discerned, the first one corresponding to a region near the minimum of the current and the second for larger

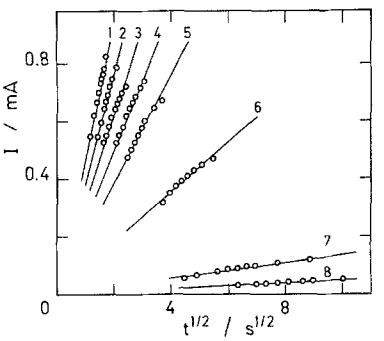

Fig. 5. Plot of I against $t^{\frac{1}{2}}$ for transients obtained for the 2.2 mol dm^{-3} KOH solution. Potential applied (mV): 1, −867; 2, −871; 3, −875; 4, −880; 5, −883; 6, −885; 7, −887; 8, −889.

Table 1. Dependence of the slopes of the $I\text{–}t^{3/2}(m_p)$ *and* $I\text{–}t^{1/2}(m_i)$ *plots on the KOH concentration and the overpotential applied*

E *(mV)*[a]	η *(mV)*	c_{KOH} *(M)*	$10^2\ m_i$ *(mA s$^{1/2}$)*	$10^2\ m_p$ *(mA s$^{3/2}$)*
−875	7	1.0	0.67	0.21
−876	6	1.0	0.39	0.10
−877	5	1.0	0.30	0.06
−879	3	1.0	0.24	0.03
−873	14	1.2	1.65	0.77
−875	12	1.2	0.96	0.30
−877	10	1.2	0.92	0.29
−879	8	1.2	0.73	0.20
−881	6	1.2	0.45	0.09
−883	4	1.2	0.39	0.05
−868	23	1.4	23.92	25.70
−870	21	1.4	22.41	25.27
−875	16	1.4	20.35	10.06
−878	13	1.4	12.39	3.76
−880	11	1.4	5.35	0.61
−883	8	1.4	3.81	0.27
−885	6	1.4	1.67	0.01
−887	4	1.4	0.45	0.01
−868	29	1.7	34.16	67.30
−870	27	1.7	32.88	33.66
−875	22	1.7	18.69	9.68
−878	19	1.7	11.54	4.79
−880	17	1.7	8.87	2.77
−883	14	1.7	6.07	0.87
−885	12	1.7	4.01	0.39
−887	10	1.7	1.34	0.07
−868	33	2.0	67.59	162.19
−870	31	2.0	67.33	133.46
−875	26	2.0	56.34	98.22
−878	23	2.0	48.65	44.62
−880	21	2.0	30.75	17.00
−883	18	2.0	16.13	4.99
−885	16	2.0	9.69	1.06
−887	14	2.0	5.73	0.36
−890	11	2.0	0.75	0.01
−867	37	2.2	46.35	72.53
−871	33	2.2	38.67	39.47
−875	29	2.2	31.39	31.18
−880	24	2.2	24.41	9.07
−883	21	2.2	19.51	4.82
−885	19	2.2	8.82	0.84
−887	17	2.2	1.34	0.19
−889	15	2.2	0.57	0.03

[a] Versus $Hg/HgO, KOH_{sln}$.

times, in agreement with Equations 5 and 6. The values of the slopes calculated for these latter plots are shown in Table 1 as a function of the potential applied and the KOH concentration. As shown, for all the concentrations used and a certain set overpotential, the values of these slopes decrease with increasing concentration of the electrolyte. On the other hand, when the overpotential decreases, the slope of the corresponding plots also decreases, this decrease being more pronounced for the I versus $t^{3/2}$ plots than for the I versus $t^{1/2}$ plots.

On the other hand, Equations 5 and 6 do not permit interpretation of the maximum of the current found in the potentiostatic curves, because these equations are only valid for short

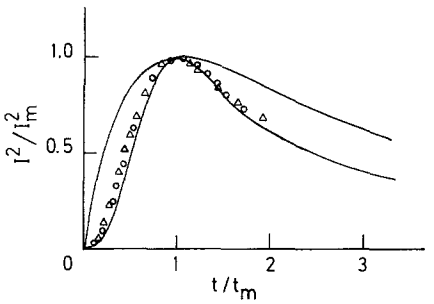

Fig. 6. Non-dimensional I^2/I_m^2 versus t/t_m plots for transients obtained for the 1.2 mol dm^{-3} KOH solution for −875 (○) and −883 (△) mV. The continuous lines correspond to equations 7 and 8 for instantaneous (upper curve) and progressive (lower curve) nucleation, respectively.

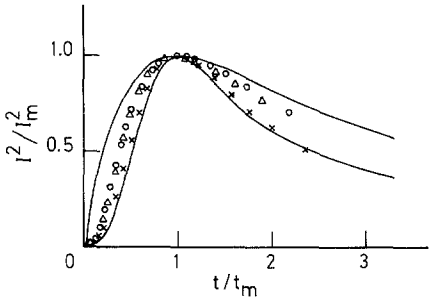

Fig. 7. Same as Fig. 6 but for 2.2 mol dm^{-3} KOH solution and potentials applied (mV): −883 (○), −880 (△) and −871 (×).

times. When the nuclei are growing, a moment arrives at which the diffusion zones overlap and the only material that contributes to the growth of the film is that arriving at the electrode in a perpendicular direction. In the latter situation, the diffusion of material towards the nuclei surface can be expressed in terms of a semi-infinite linear diffusion to that fraction of the electrode surface embraced within the perimeter of the growing diffusion zones. On this basis, and taking into account the overlap of the diffusion zones of the nuclei, Scharifker and Hills [18] have deduced equations describing the current transients for instantaneous and progressive nucleation. In each case, the current passes through a maximum and then approaches the limiting diffusion current to a planar electrode. The final equations resulting from the analysis of the maximum current, in reduced coordinates, are

$$I^2/I_m^2 = \frac{1.9542}{t/t_m}\{1 - \exp[-1.2564(t/t_m)]\}^2 \quad (7)$$

for an instantaneous nucleation and

$$I^2/I_m^2 = \frac{1.2254}{t/t_m}\{1 - \exp[-2.3367(t/t_m)^2]\}^2 \quad (8)$$

for a progressive nucleation. Thus, the transients can be presented in a non-dimensional form by plotting I^2/I_m^2 versus t/t_m and compared with theory through Equations 7 and 8 for instantaneous and progressive nucleation, respectively. The curves corresponding to the KOH solutions of concentrations 1.2 and 2.2 mol dm^{-3} are represented in Figs 6 and 7. These latter plots show how, for all the concentrations used and times near the minimum value of the current, the experimental points can be fitted to the theoretical curve given by Equation 8, which corresponds to a progressive nucleation. For larger times, a certain dependence of the experimental curves on the electrolyte concentration is observed. Thus, for 1.0 and 1.2 mol dm^{-3} KOH solutions a considerable overlap with the theoretical curve predicted by Equation 8 is obtained (cf. Fig. 6), while for the other concentrations employed, the experimental curves show a mixing of both types of nucleation (progressive and instantaneous), being more appreciable when the overpotential decreases (cf. Fig. 7).

Due to the fact that for times somewhat greater than that corresponding to the minimum of current, the log I versus log t plots exhibit a slope of $\frac{1}{2}$, it is possible that, for these values of time, instantaneous nucleation prevails. This effect can be interpreted as a consequence of a change in the type of nucleation, this change being more appreciable when the overpotential decreases, as can be deduced from the values of the slopes for progressive nucleation, m_p, and for instantaneous nucleation, m_i, which are shown in Table 1. The values of m_p decrease more rapidly than m_i when the overpotential decreases, this fact being in agreement with the results corresponding to the (I^2/I_m^2) versus (t/t_m) plots (cf. Fig. 7).

Therefore, it is possible to postulate, for the formation of the oxidized species of cadmium, a

kinetic model of electrocrystallization with a three-dimensional, hemispherical growth controlled by diffusion of the species toward the growth centres, with a progressive nucleation for times near the minimum value of current and instantaneous nucleation for times somewhat greater. It is possibly to justify this change in the type of nucleation. For short times the nuclei are formed and grow independently of each other. However, while these nuclei are growing, the diffusion zones corresponding to different nuclei overlap. It is expected that the overlapping decreases the nucleation rate and then, if in the overlapping zones there is a certain active centre which could be transformed in a nucleus, it will not be formed. This would indicate that, while the overlapping zones increase, the number of potentially active centres which will not be transformed in nuclei is greater than in the absence of overlapping. If this is the case, a certain range of time in which the growth of the nuclei previously formed predominates would exist. In this way, a change in the predominance of the type of nucleation will take place. Thus, it seems that the nucleation is progressive until the sites are exhausted or deactivated by overlapping of the diffusion zones.

On the other hand, for a set value of the overpotential the relation between the slope of the I versus $t^{3/2}$ plots (Equation 6), m_p, and the I versus $t^{1/2}$ plots (Equation 5), m_i, which can be expressed as

$$\frac{m_p}{m_i} = \frac{3}{2}\left(\frac{AN_\infty}{N}\right) \qquad (9)$$

shows the effect of changing the pH of the solution on the kinetics of nuclei formation. Therefore, the double logarithmic relation between m_p/m_i and the activity of the electrolyte [19], has been plotted for low values of the overpotential. In this case, straight lines with slopes of approximately -4 are found (Fig. 8). Consequently, for low overpotentials it is possible to write

$$AN_\infty/N = ka_{KOH}^{-n} \qquad (10)$$

where k is a parameter which depends on the overpotential. This indicates that the relation between the number of active centres which are transformed progressively in nuclei and the number of active centres which are transformed instantaneously in nuclei decreases when the activity of the electrolyte increases, in agreement with the above discussion (cf. Fig. 7).

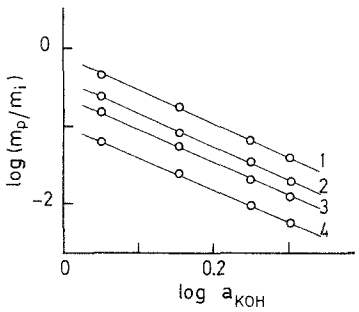

Fig. 8. Plots of log (m_p/m_i) versus log a_{KOH}. Overpotential (mV): 1, 15; 2, 12; 3, 10; 4, 8.

References

[1] J. A. Garrido, E. Pérez and J. Virgili, *An. Quím.* **78A** (1982) 268.
[2] *Idem, ibid.* **78A** (1982) 275.
[3] F. Centellas, J. A. Garrido, E. Pérez and J. Virgili, *ibid.* **79A** (1983) 656.
[4] D. W. Shoesmith, S. Sunder, M. G. Bailey, G. J. Wallace and F. W. Stanchell, *J. Electroanal. Chem.* **143** (1983) 153.
[5] F. Centellas, J. A. Garrido, A. Gironés, E. Pérez and J. Virgili, *An. Quím.* **80A** (1984) 193.
[6] F. Centellas, J. L. Fernández, J. A. Garrido, E. Pérez and J. Virgili, *ibid.* **81A** (1985) 452.
[7] R. D. Armstrong, E. H. Boult, D. F. Porter and H. R. Thirsk, *Electrochim. Acta* **12** (1967) 1245.
[8] M. W. Breiter and W. Vedder, *Trans. Faraday Soc.* **63** (1967) 1042.
[9] Y. Okinaka and C. M. Whitehurst, *J. Electrochem. Soc.* **117** (1970) 583.
[10] K. Huber and S. Stucki, *Helv. Chim. Acta* **51** (1968) 1343.
[11] E. J. Casey and C. L. Gardner, *J. Electrochem. Soc.* **122** (1975) 851.
[12] D. W. Shoesmith, T. E. Rummery, D. Owen and M. Lee, *ibid.* **123** (1976) 790.
[13] M. Fleischmann and H. R. Thirsk, in 'Advances in Electrochemistry and Electrochemical Engineering' (edited by P. Delahay), Vol. 3, Interscience, New York (1963) chap. 3.
[14] D. D. Macdonald, in 'Transient Techniques in Electrochemistry', Plenum Press, New York (1977) chap. 8.
[15] M. Y. Abyaneh, *Electrochim. Acta* **27** (1982) 1329.
[16] R. Greef, R. Peat, L. M. Peter, D. Pletcher and J. Robinson, in 'Instrumental Methods in Electrochemistry', Southampton Electrochemistry Group, Ellis Horwood, Chichester (1985) chap. 9.
[17] G. J. Hills, D. J. Schiffrin and J. Thompson, *Electrochim. Acta,* **19** (1974) 657.
[18] B. Scharifker and G. J. Hills, *ibid.* **28** (1983) 879.
[19] R. Parsons, 'Handbook of Electrochemical Constants', Butterworths, London (1959).